

Edge electric-field profiles of H-mode plasmas in the JFT-2M tokamak

journal or publication title	Physical Review Letters
volume	Vol.65
number	No.11
page range	pp.1364 - 1367
year	1990-09-01
URL	http://hdl.handle.net/10655/86

doi: 10.1103/PhysRevLett.65.1364

Edge Electric-Field Profiles of *H*-Mode Plasmas in the JFT-2M Tokamak

K. Ida and S. Hidekuma

National Institute for Fusion Science, Nagoya, 464-01, Japan

Y. Miura, T. Fujita, M. Mori, K. Hoshino, N. Suzuki, T. Yamauchi, and JFT-2M Group

Japan Atomic Energy Research Institute, Naka-machi, Naka-gun, Ibaraki, 319-11, Japan

(Received 13 March 1990)

The structure of the edge radial electric field E_r , inferred from the poloidal rotation velocity is compared with that of the particle and thermal transport barrier for *H*-mode plasmas in JFT-2M. Both E_r and its gradient $\partial E_r/\partial r$ in the thermal transport barrier are found to become more negative at the *L-H* transition. On the other hand, $\partial E_r/\partial r$ is more positive outside of the separatrix. The shear of the radial electric field and poloidal rotation velocity in the *H* mode is localized within the order of an ion poloidal gyroradius near the separatrix, in the region of ion collisionality $\nu_{*i} \approx 20-40$.

PACS numbers: 52.55.Fa, 52.55.Pi, 52.70.Kz

Since the *H*-mode plasma was discovered in ASDEX,¹ it has been observed in many tokamaks.²⁻⁵ Several theoretical models on the transition from *L*-mode to *H*-mode plasmas have been presented.⁶⁻¹¹ Recently, a radial electric field (E_r) near the plasma periphery has been found both experimentally and theoretically to play an important role in the *L-H* transition.¹²⁻¹⁹ A more negative radial electric field was observed a few ms before the *L-H* transition in DIII-D (Ref. 12), and a decrease in particle transport was observed with negative E_r , by driving a radial current, in the Continuous Current Tokamak.¹³ Theoretical models associated with the radial electric field have been proposed to explain the *L-H* transition.¹⁴⁻¹⁷ However, the predicted change of the gradient of the radial electric field ($\partial E_r/\partial r$) is different between the models. In Shaing and Crume's model,¹⁶ the poloidal flow velocity changes at the *L-H* transition and the corresponding radial electric field E_r becomes more negative and $\partial E_r/\partial r$ becomes more positive, hence suppressing the fluctuations. On the other hand, Itoh and Itoh's model¹⁷ predicts positive values of $\partial E_r/\partial r$ in the *L* mode and negative values of $\partial E_r/\partial r$ in the *H* mode, and that this negative $\partial E_r/\partial r$ reduces the banana width of the ions and the electron anomalous flux by the improved microstability. Thus it is crucial to measure the gradient or profile of the radial electric field for *L*- and *H*-mode plasmas in tokamaks.

In this paper we present the radial electric-field profile and temperature gradient profile a few cm inside the separatrix where the transport barrier is produced in *H*-mode plasmas in JFT-2M.⁵ The radial electric-field profiles are inferred from poloidal and toroidal rotation velocity profiles and ion pressure profiles using the ion-momentum-balance equation,

$$E_r = \frac{\partial p_i}{eZ_i n_i \partial r} - (B_\theta v_\varphi - B_\varphi v_\theta),$$

where Z_i , p_i , and n_i are the ion charge, pressure, and density, B_φ and B_θ are the toroidal and poloidal magnetic

fields, and v_φ and v_θ are the toroidal and poloidal rotation velocities. The toroidal rotation velocity, ion temperature, and fully stripped carbon density profiles are measured using a multichannel charge-exchange-spectroscopy technique^{18,19} at C VI 5292 Å with toroidal arrays (two sets of 34 channels) with a spatial resolution of 1 cm. The poloidal rotation velocity and edge ion temperature profiles are measured using the intrinsic radiation of C VI at 5292 Å with poloidal arrays (two sets of 23 channels), which do not view across the beam line and view only the plasma periphery with a spatial resolution of 4 mm. In order to avoid the line-of-sight integration problem, a wavelength-resolved Abel inversion¹⁸ is used to obtain the local ion temperature and poloidal rotation velocity from the poloidal arrays. These two sets of toroidal and poloidal arrays view the plasma in opposite directions to define the zero reference for Doppler-shift measurements.

The electron temperature profile and its gradient profile are measured with an electron-cyclotron-emission (ECE) radiometer to investigate the location of the thermal transport barrier. The electron temperature is obtained from the intensity of the ECE with some correction associated with optical thickness and reflection coefficient at the wall. The spatial resolution of the measurements set by the frequency bandwidth of the detector is 3 mm. The bulk electron density (n_e) and temperature (T_e) are measured with Thomson scattering and the edge n_e and T_e profiles are measured with an electric probe from 5 mm inside to 30 mm outside of the separatrix. The uncertainty in the position of the separatrix calculated with an equilibrium code is estimated to be 5 mm.

Figure 1 shows the time evolution of the poloidal rotation velocity for a plasma with a current of 250 kA, a toroidal field of 1.24 T, and q_w of 2.8 in a single-null-divertor configuration. The neutral beam is injected at 700 ms in the codirection with a power of 0.7 MW. A jump in the poloidal rotation velocity at the *L-H* transi-

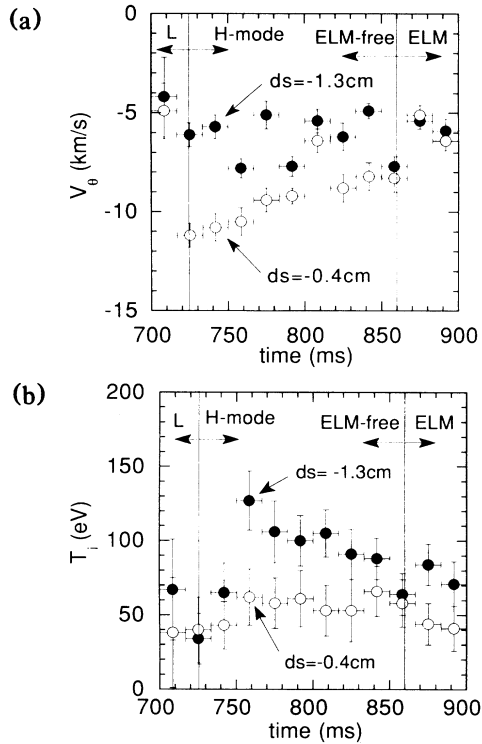


FIG. 1. Time evolution of (a) poloidal rotation velocity and (b) ion temperature at 0.4 cm (open circles) and 1.3 cm (closed circles) inside the separatrix. The L - H transition occurs at $t = 725$ ms.

tion is observed at 0.4 cm inside the separatrix, while a significant increase of ion temperature is observed at $d_s = -1.3$ cm, further inside the plasma. The poloidal rotation velocity increases in the electron diamagnetic direction in the H mode regardless of the direction of the plasma current and neutral-beam injection. The change of poloidal rotation velocity occurs prior to the change of ion temperature and is fairly localized near the separatrix, while the sharp gradient of the ion temperature is also observed further inside. In the H mode with the edge localized mode, no poloidal-rotation-velocity shear is observed; however, a steep gradient of the ion temperature is observed. A strong shear of the poloidal rotation velocity is observed in the region of $|a - r| < \rho_p \approx 1.3$ cm. The profiles of ion and electron temperature, density, and poloidal and toroidal rotation velocity are measured in detail before ($t = 710$ ms) and after ($t = 740$ ms) the L - H transition to derive radial electric-field profiles, and are shown in Figs. 2 and 3(a).

As shown in Fig. 3(b), the electric-field profiles for L -mode and H -mode plasmas are calculated from rotation velocities and pressure gradients of carbon using a momentum-balance equation for C^{5+} , not bulk ions. Although no difference in rotation velocity between different ion species (He^{2+} and O^{8+}) has been observed in steady-state plasma,²⁰ there is no guarantee that bulk ions rotate with the same velocity as carbon, when the

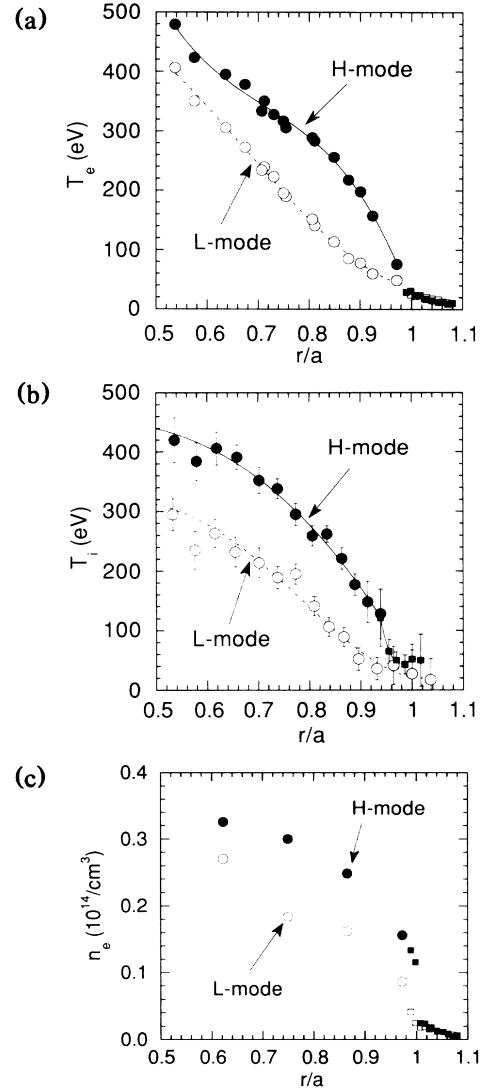


FIG. 2. Radial profiles of (a) electron temperature measured with ECE radiometer (circles) and electric probes (squares), (b) ion temperature measured with toroidal (circles) and poloidal (squares) arrays, and (c) electron density measured with Thomson scattering (circles) and electric probes (squares), for L -mode ($t = 710$ ms, open symbols) and H -mode ($t = 740$ ms, closed symbols) plasmas, where r/a is a normalized minor radius.

plasma changes quickly at the L - H transition. The electric field becomes more negative in the H mode, due to the increase of poloidal rotation velocity in the electron diamagnetic direction. The gradient of the electric field inside the separatrix, $d_s = -0.7$ cm, becomes more negative, -80 ± 10 V/cm², in the H mode. The ion and electron thermal transport barrier is found at 1–2 cm inside the separatrix. On the other hand, the steep gradients of electron density and brightness of C VI emission are concentrated near the plasma edge within 0.5 cm of the separatrix, as shown in Fig. 4. The absolute values of the gradient of electron density measured with electric

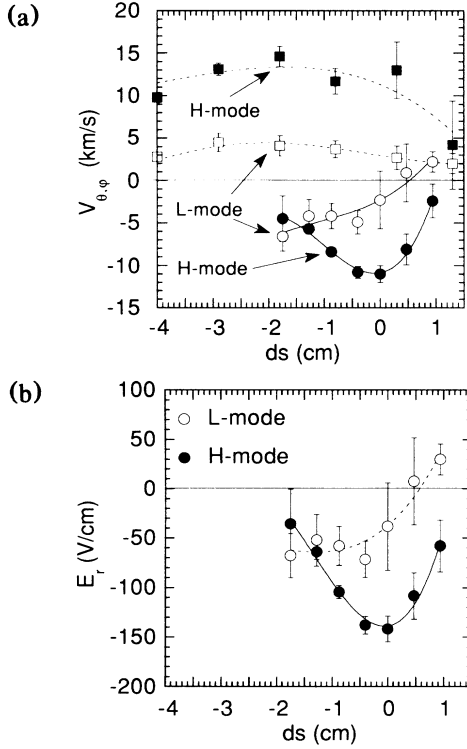


FIG. 3. Radial profiles of (a) poloidal (circles) and toroidal (squares) rotation velocities and (b) radial electric field, as a function of the distance from the separatrix, for *L*-mode ($t=710$ ms, open symbols) and *H*-mode ($t=740$ ms, closed symbols) plasmas. d_s is negative inside and positive outside of the separatrix.

probes have an uncertainty of a factor of 2; however, the relative values are accurate enough to measure the location of steep density gradients. The brightness of C VI emission is roughly proportional to the product of electron density and C^{5+} density, since the excitation rate in the visible region has a weak temperature dependence. We note that the steep gradients of density and temperature are produced in different regions of the plasma. This is partly due to the different locations of the sources. The particle source is concentrated near the plasma edge, since it does not penetrate deeply into the plasma with a density of more than $1 \times 10^{13}/\text{cm}^3$. On the other hand, the heat sources of both the Ohmic input and the tangential neutral beam are peaked at the plasma center. These measurements (Figs. 3 and 4) seem to indicate that the improvement of thermal transport correlates with the negative $\partial E_r/\partial r$. However, these measurements do not exclude the possibility that the more negative electric field itself, and not the gradient, is important in the *L-H* transition.

It is important to compare the measured plasma parameters such as poloidal rotation velocity, electric field, and bulk ion pressure gradient with the Shaing-Crume and Itoh-Itoh models. The bulk ion temperature is assumed to be the same as the carbon temperature, and the

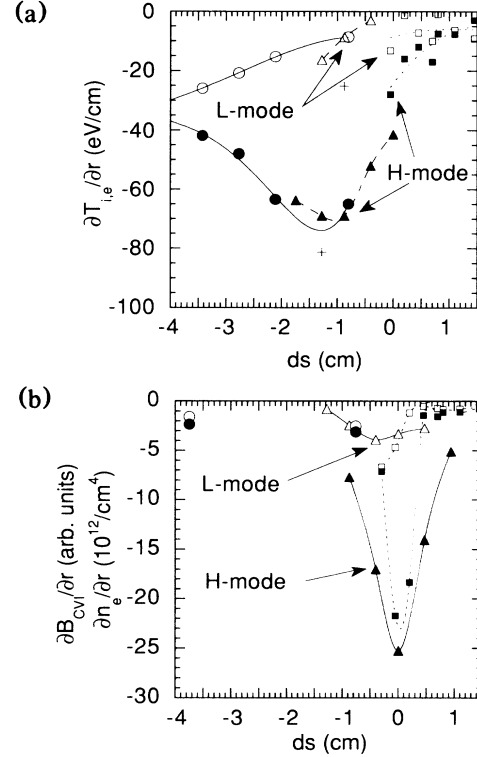


FIG. 4. Gradients of (a) electron temperature measured with ECE radiometer (circles) and electric probes (squares) and ion temperature (plusses for $t=740$ ms, triangles for $t=760$ ms), and (b) electron density measured with Thomson scattering (circles) and electric probes (squares) and brightness of C VI emission (triangles), as a function of the distance from the separatrix for *L*-mode ($t=710$ ms, open symbols) and *H*-mode ($t=740$ ms, closed symbols) plasmas.

ion density profile is estimated with the electron density profile and the carbon density profile,¹⁹ which is a dominant impurity in JFT-2M. The poloidal-rotation parameter $U_{p,m}$ [$=v_{\theta}B/v_{\varphi}B_{\theta}+\lambda_p/2$, $\lambda_p=\rho_p(\partial p_i/\partial r)/\rho_i$] changes from 2.1 ± 0.4 to 3.4 ± 0.2 at the *L-H* transition 0.9 cm inside the separatrix. This change of poloidal rotation at the *L-H* transition agrees with the prediction of Shaing and Crume's model¹⁶ within a factor of 2 or 3. The ion collisionality ν_{*i} at 0.7 cm inside the separatrix decreases from 44 ± 7 (*L* mode) to 22 ± 10 (*H* mode). The measured rotation parameter and critical ν_{*i} values do not agree with the critical value of ν_{*i} (≈ 1.5) and $U_{p,m}$ before the *L-H* transition (≈ 0.7) in their model. The large value of the critical ν_{*i} measured in JFT-2M may be explained with Shaing and Crume's model by including the additional effect of fast ion loss.²¹ It is also interesting to evaluate the strength of the gradient of the radial electric field, $\partial E_r/\partial r$, since it can affect the ion orbit and change the banana width of the ions by a factor of $(|1-u_g|+C\varepsilon)^{-1/2}$, where ε and C are an inverse aspect ratio and a numerical coefficient.^{15,22} The shear parameter of the electric field u_g , defined by $\rho_p(\partial E_r/$

$\partial r)/v_{th}B_\theta$, is 0.3 ± 0.3 for the L mode and -1.6 ± 0.2 for the H mode at 0.7 cm inside the separatrix. The gradient of the electric field measured in the H mode is large enough to change the banana width. This shear parameter u_g is 1.0 in the L mode and -2.3 in the H mode in Itoh and Itoh's model.¹⁷ The pressure-gradient parameter λ [$= -(T_e/T_i)\rho_p\{(\partial n_e/\partial r)/n_e + \alpha(\partial T_e/\partial r)/T_e\}$] defined in Itoh and Itoh's model changes from 0.5 to 1.3 at the L - H transition and is consistent with the critical value of their model ($\lambda_c \approx 1$). We observe qualitative agreement of characteristic parameters in the L - H transition with Itoh and Itoh's model and Shaing and Crume's model. However, both models are point models and do not fully explain the structure of the edge electric field, the negative $\partial E_r/\partial r$ in the thermal transport barrier, and the positive $\partial E_r/\partial r$ further outside.

In conclusion, both E_r and $\partial E_r/\partial r$ become more negative in the thermal barrier, 1–2 cm inside the separatrix, in the L - H transition. Positive $\partial E_r/\partial r$ is observed outside of the separatrix for both L - and H -mode plasmas.

We would like to thank S.-I. Itoh, K. Itoh, and K. Toi [National Institute for Fusion Science (NIFS)] and K. C. Shaing (ORNL) for their useful discussions. Comments by T. Leonard (GA Technologies) are acknowledged. We also thank T. Matsuda [Japan Atomic Energy Research Institute (JAERI)] and M. Kojima (NIFS) for their support with data acquisition. The continuous encouragement of H. Maeda (JAERI), Y. Hamada (NIFS), and K. Matsuoka (NIFS) is acknowledged.

- ¹F. Wagner *et al.*, Phys. Rev. Lett. **49**, 1408 (1982).
- ²S. M. Kaye *et al.*, J. Nucl. Mater. **121**, 115 (1984).
- ³M. Nagami *et al.*, Nucl. Fusion **24**, 183 (1984).
- ⁴A. Tanga *et al.*, Nucl. Fusion **27**, 1877 (1987).
- ⁵S. Sengoku *et al.*, Phys. Rev. Lett. **59**, 450 (1987).
- ⁶T. Ohkawa *et al.*, Phys. Rev. Lett. **51**, 2101 (1983).
- ⁷F. L. Hinton Nucl. Fusion **25**, 1457 (1985).
- ⁸H. P. Furth, Plasma Phys. Controlled Fusion **28**, 1305 (1986).
- ⁹N. Ohyabu *et al.*, Nucl. Fusion **26**, 593 (1986).
- ¹⁰C. M. Bishop, Nucl. Fusion **26**, 1063 (1986).
- ¹¹T. S. Hamm and P. H. Diamond, Phys. Fluids **30**, 133 (1987).
- ¹²K. H. Burrell *et al.*, Plasma Phys. Controlled Nucl. Fusion Res. **31**, 1649 (1989).
- ¹³R. J. Taylor *et al.*, Phys. Rev. Lett. **63**, 2365 (1989).
- ¹⁴S.-I. Itoh and K. Itoh, Phys. Rev. Lett. **60**, 2276 (1988).
- ¹⁵S.-I. Itoh and K. Itoh, Nucl. Fusion **29**, 1031 (1989).
- ¹⁶K. C. Shaing and E. C. Crume, Jr., Phys. Rev. Lett. **63**, 2369 (1989).
- ¹⁷S.-I. Itoh and K. Itoh, National Institute for Fusion Science Research Report No. NIFS-4, 1990 (unpublished).
- ¹⁸K. Ida and S. Hidekuma, Rev. Sci. Instrum. **60**, 867 (1989).
- ¹⁹K. Ida, T. Amano, K. Kawahata, O. Kaneko, and H. Tawara, Nucl. Fusion **30**, 665 (1990).
- ²⁰K. H. Burrell, R. J. Groebner, H. St. John, and R. P. Seraydarian, Nucl. Fusion **28**, 3 (1988).
- ²¹K. C. Shaing (private communication).
- ²²F. L. Hinton in *Proceedings of the Sherwood Controlled Fusion Theory Conference, San Diego, 1987* (Science Applications, San Diego, 1987).